Tests of Impedance Theories for a Transmitting Dipole in an Ionospheric Plasma

H. GORDON JAMES

Abstract—**The voltage at the output of the sounder transmitter in both of the International Satellites for Ionospheric Studies (ISIS) ionospheric spacecraft is routinely recorded over the entire frequency range of 0.1–20 MHz. The observed dependence of the output voltage on the sounder frequency is determined by the values of the local plasma parameters, of which there is a considerable range in the ISIS data. Impedance theories for an ionospheric dipole have been tested by comparing observed curves of voltage versus sounder frequency with computed curves based on those theories. In cases where the plasma frequency is low, around 0.1 MHz, a realistic curve is obtained using standard vacuum dipole theory. For higher plasma frequencies, the observed response departs significantly from the low-density case at frequencies close to the electron characteristic frequencies. For fixed working frequency and plasma parameters, the voltage exhibits a slight dependence on antenna orientation. Attempts to explain these results for higher plasma frequencies using a transmission-line theory have qualified success when a vacuum sheath of 1-m radius is assumed. The need for a large sheath is just one kind of evidence that the sounder *rf* fields profoundly change the nature of the plasma near the dipole.**

I. INTRODUCTION

A PEAK RF voltage detector was included in the design of the output of the International Satellite for Ionospheric Studies (ISIS) I and ISIS II sounder power amplifiers as a means of monitoring the transmitter and verifying correct operation after launch. Examination of data gathered subsequently has revealed that the monitor voltage responds consistently to changes in the ambient ionospheric plasma and hence could probably be used to study the behavior of an antenna in a plasma.

Much experimental and theoretical research has been carried out in the field of antenna plasma properties, and the reader is referred to the literature [1]. Nevertheless, the ISIS sounder experiment has a unique combination of characteristics which indicate that plasma antenna investigations using it would be useful. First, because sounder sweep frequencies near 1 MHz can correspond, at the same time, to characteristic frequencies of the plasma and to the frequency at which the length (73 m) of the dipole equals a half-wavelength in the medium, ISIS permits the study of the finite dipole in a frequency range where plasma effects are expected to be important. Second, the ISIS II altitude of 1400 km corresponds to an electron gyrofrequency also close to 1 MHz, and this means that the various plasma frequency domains can be clearly resolved. Third, the ISIS transmitter is a comparatively powerful signal source (400 W) and can be used to investigate nonlinear effects associated with intense radio fields in plasmas; study of the monitor response may therefore be of use in the planning of future space radio transmitters.

Theoretical analysis of this combination is very difficult. Although various published theoretical works address some of the aspects of this situation, a complete understanding does not appear to have developed. It is hoped that this work may stimulate further investigation in this field.

The ISIS output monitor is not an ideal plasma measurement device. The monitor records only the magnitude of the power amplifier voltage, at a point that is separated from the antenna terminals by a matching network. The object of this work is to test antenna impedance theories by comparing the observed curve of output voltage versus frequency with a theoretical calculation. Because only the voltage magnitude is measured, the complex antenna impedance cannot be inferred directly. In cases of disagreement, the only conclusion that can definitely be made is that the theory is incorrect.

In this paper a number of output voltage versus frequency plots are displayed. The dependence of the response on plasma parameters and antenna orientation is discussed. The theory has been evaluated using a computer program that is based on the antenna matching circuit and an equivalent circuit for the power amplifier; it also permits a choice of theoretical expressions for the impedance of the finite dipole in a plasma. A vacuum impedance theory agrees well with the relevant observations, whereas a plasma impedance theory has qualified success when compared with observations at frequencies near the electron characteristic frequencies.

II. SPACECRAFT DETAILS

ISIS I and ISIS II are multiinstrument ionospheric spacecraft launched in 1969 and 1971, respectively [2]. The apogee, perigee, and inclination of the ISIS I orbit are 3520 km, 570 km, and 88°, respectively. ISIS II is in a nearly circular orbit at about 1400 km altitude with an inclination of 89°.

The pertinent parts of the ISIS I sounder system [3] are shown in Fig. 1. In ISIS II, the 100-W power amplifier is replaced by a second 400-W amplifier for redundancy; otherwise, the ISIS II system is the same. In the power amplifier, a square gate pulse lasting approximately 100 μs modulates the input from the RF generator, and after several stages of amplification the pulse can deliver 400 W into a matched resistive load of 400 Ω at 1.5 MHz. The driver and balanced amplifier in the 400-W power amplifier in Fig. 1 is shown in detail by Franklin and Maclean's [3, fig. 14] while the output amplifier and driver includes a common-base stage driving the final stage shown in [3, fig. 15]. The 100-W power amplifier is different in that its output amplifier and driver do not have the six-transistor output stage shown in [3, fig. 15]. The basic sounder cycle comprises the 100-μs transmitted pulse followed by a receiver listening time of about 30 ms. Parameters of the sounder operation, such as power amplifier, sweep mode, and ionogram frame length, are selected by telecommand. The sounder mode used in the present work provides a continuous series of ionograms in the frequency range between 0.1 MHz and either 10 or 20 MHz.

The data reported here come from the monitor detector

Manuscript received April 1, 1979; revised November 1, 1979.

The author is with the Communications Research Centre, Department of Communications, Ottawa, ON, Canada K2H 8S2.

0018-926X/80/0900-0623$00.75

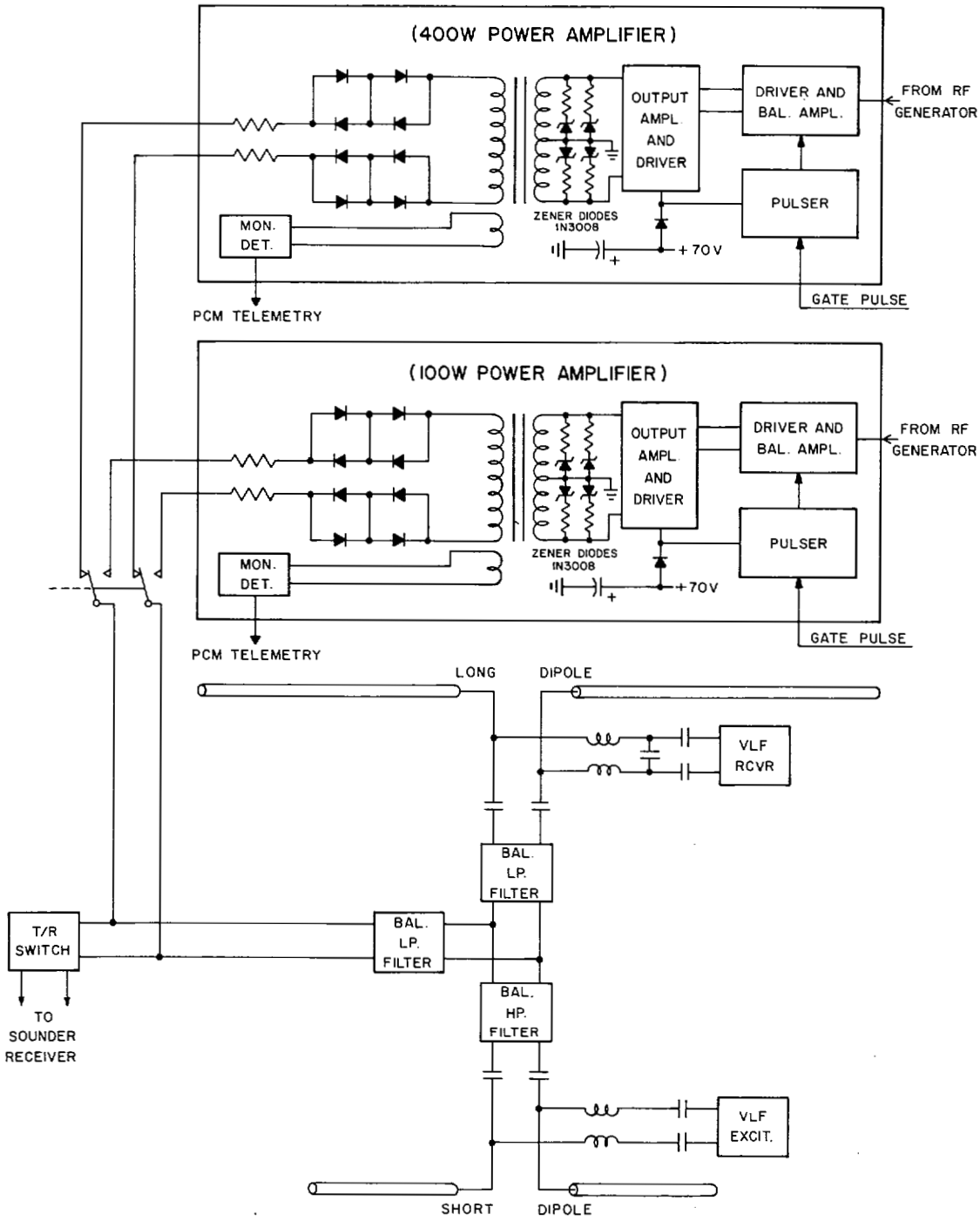

Fig. 1. Schematic of ISIS I radio equipments. Output amplifier in 400-W amplifier has one more stage of amplification than 100-W amplifier. ISIS II system is same except that a second 400-W amplifier replaces 100-W amplifier on ISIS I.

which is fed by a pickup coil on the secondary side of the last transformer in the amplifier, as shown in Fig. 1. In the monitor, the pulse envelope is detected and the voltage held nearly constant (RC = 267 ms) until the next pulse. This voltage lies in the range 0–5.12 V and is sampled twice per second by the pulse-code modulation (PCM) encoder which uses 8-bit words, and which therefore gives 256 digital levels between 0 and 5.12 V. When the detected voltage exceeds 5.12 V, this value of 5.12 is encoded. Prior to spacecraft launch, calibration procedures established the linear proportionality, $a = V_m/V_S$, between the peak voltage across the secondary of the amplifier output transformer V_S and the monitor voltage V_m; in ISIS I and ISIS II, a is 0.0040 and 0.0051, respectively.

Fig. 1 also indicates that the measurement point is separated from the antenna terminals by isolating diodes and resistances in the amplifier, balanced filters comprising the crossover network, and dc blocking capacitors. The balanced filters are composed of passive tuned LC circuits and have a crossover frequency of 5 MHz. The transmit–receive switch can be represented by inductances across the lines while the VLF units, and their associated low-pass filters can be neglected in the analysis.

The sounder dipoles are beryllium-copper storable extendible member (STEM) elements of 13-mm diameter and have tip-to-tip lengths of 73.2 and 18.8 m. Both ISIS I and ISIS II are spin stabilized at approximately 3 r/min, with the crossed

sounder dipoles in the spacecraft equatorial plane. Their instantaneous orientation can be calculated from magnetometer and solar sensor recordings.

Satellite data are recorded in real time by ground telemetry. Subsequent processing requires digital techniques for the various PCM data, such as the monitor voltage and orientation information, and FM techniques for the ionograms from which plasma parameters are scaled. The PCM format also contains information flags on the sounder frequency markers. Frequencies are assigned to voltage data by interpolating between frequency markers.

III. EQUIVALENT CIRCUIT CALCULATIONS AND DATA ANALYSIS

The amplifier response was analyzed using the equivalent circuit of Franklin and Maclean [3, fig. 16]. The 400-W amplifier produces a peak current i_s of 9.2 A. It is evident from the data that the clamping Zener diodes of type 1N3008 at the output amplifier in Fig. 1 play an important role in determining the shape of the monitor response; a nonlinear resistance with the current–voltage characteristic in Fig. 2, based on nominal published values, was added in parallel with the load R_L in the equivalent circuit. R_L accounts for both the matching network and antenna impedances and is generally complex.

Preliminary calculations of the theoretical response of the output voltage V_S were performed using a rigorous nonlinear transient analysis to evaluate the importance of the finite spectral bandwidth of the pulse and the severe clamping action of the Zener diodes at a high output voltage. The details of the theoretical voltage transient waveform during the first several RF cycles were found to vary considerably as the parameters of the theoretical dipole impedance were changed. However, in all instances the voltage achieved a steady-state nonlinear waveform in less than 10 RF cycles, or 0.1 ms in the longest case. This delay after the start of the pulse is very short compared with the various times at the which the PCM encoder samples the monitor; sampling times are of the order of several milliseconds. Therefore, only a steady-state solution is required.

The I–V characteristics of the 1N3008 diodes in Fig. 2 are nominal; precise details from the ISIS flight models are unavailable. Use of nominal values means that the steady-state monitor voltage values exceeding 118 V have uncertainties of about ten percent, whereas below it they are accurate to a few percent. This error dominates the uncertainties arising from the matching network or other parts of the power amplifier.

The analysis procedure assumes a theoretical expression for the dipole impedance. The impedance presented to the equivalent circuit by the combination of the antenna, and the crossover network is then calculated; this combination replaces the R_L of Franklin and Maclean [3, fig. 16]. Given the peak current i_s from the constant-current generator, the peak steady-state voltage on the output side of the last stage transformer and hence the monitor voltage are computed. The antenna theory can then be tested by comparing the theoretical and observed monitor voltage.

Data from a considerable number of spacecraft orbits were required because of the low recording rate: in a 15-s frequency sweep, the monitor is sampled only 30 times. Because the PCM recording cycle is not synchronized with the sounder sweep, responses having a smooth distribution of data points through all frequencies can be obtained only by accumulating many ionogram sweeps. Monitor voltage–frequency data from approximately 120 ISIS I passes and 70 ISIS II passes were sorted according to plasma frequency f_N, gyrofrequency f_H,

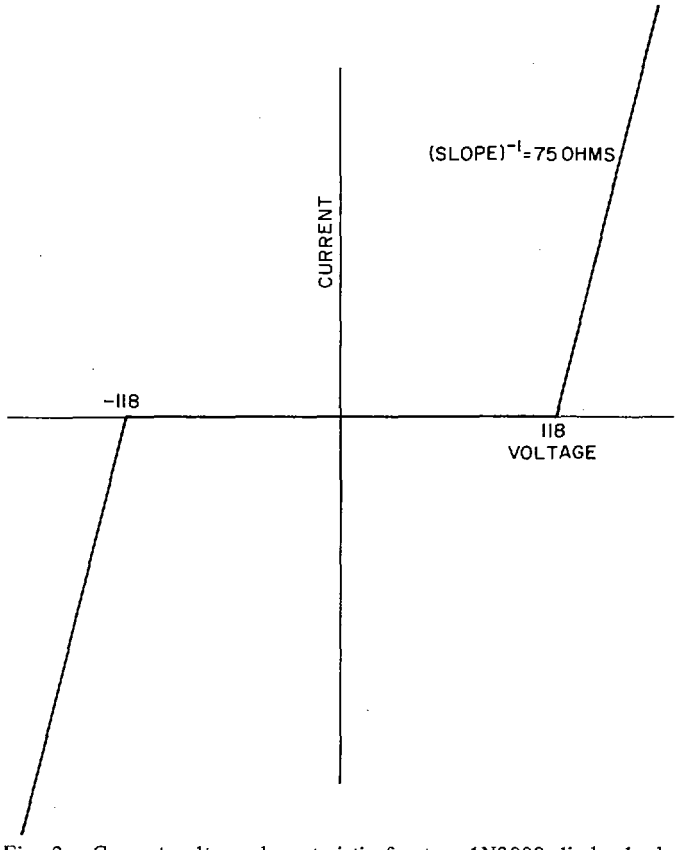

Fig. 2. Current–voltage characteristic for two 1N3008 diodes back-to-back.

and the orientation of the long dipole. The ISIS I data, coming from an elliptical orbit, provided a wider variation in f_N and f_H; they were also used in the investigation of the differences between the 100-W and 400-W amplifier responses. The ISIS II data were used to show the orientation dependence of the response.

Most of the data were recorded at mid to high latitudes and during passes when the spin vector was nearly perpendicular to the orbital plane so that the angle between the dipoles and the magnetic field swept through most of the range 0°–90°. Values of local f_N were derived from ionograms recorded simultaneously [4]. Local f_N values were set equal to the mean of the values obtained from each of the following scaled characteristics: the f_N and f_T (upper hybrid resonance frequency) spikes and the f_Z and f_X cutoff frequencies (Z mode and X mode, respectively). Here

$$f_T = \sqrt{f_N^2 + f_H^2},$$

$$f_Z = (-f_H + \sqrt{f_H^2 + 4f_N^2})/2,$$

and

$$f_X = (f_H + \sqrt{f_H^2 + 4f_N^2})/2.$$

The gyrofrequency was evaluated using a real terrestrial magnetic field model based on the GSFC POGO 3/68 coefficients [5].

Monitor voltage and frequency data points were merged and sorted into bins corresponding to small ranges of the important parameters using a computer sort processor. A range bin had to be big enough to have enough data to show clearly the response for all frequencies, yet small enough that parame-

trical variations were unimportant; range bins for the plasma characteristic frequencies and the antenna orientation angles of about 100 kHz and 30°, respectively, were chosen.

IV. RESULTS

Figs. 3–9 present voltage monitor data (dots) for a variety of conditions and compare the data with a theoretical calculation (thin line). Depending on the value of f_N, a vacuum-dipole or plasma-dipole theory was applied; these two cases are discussed in Subsections *A* and *B*. A general feature is the series of maxima and minima corresponding to swings in V_S of several hundred volts. The positions in frequency of the extrema will be seen below to be sensitively dependent on the plasma parameters for frequencies close to the plasma frequency. At frequencies of more than about twice the plasma frequency, the only significant contribution to the point spread at constant frequency comes from variations in the internal temperature of the spacecraft electronics, resulting in spreads of a few percent. This temperature effect has not been removed from the data.

A. Results for Low Plasma Density

Fig. 3 gives the ISIS II monitor response when f_N lies between 0.1 and 0.2 MHz, and the entire frequency range from 0.1 to 20.0 MHz is virtually unaffected by the plasma. The antenna impedance Z was evaluated using a simplified version of Schelkunoff and Friis' [6, expression 13-108] for the finite dipole in a vacuum:

$$Z = K_a \cdot \frac{(K_a - M)\cos(k_0 l) + j(Z_a - jN)\sin(k_0 l)}{(Z_a + jN)\cos(k_0 l) + j(K_a + M)\sin(k_0 l)} \qquad (1)$$

in which K_a is the characteristic impedance of a cylindrical dipole, $120(\log(2l/\rho) - 1)\Omega$, l is the dipole half-length, ρ is the dipole radius, k_0 is the vacuum wavenumber, and Z_a, M, and N are explicit functions depending on $\sin(k_0 l)$, $\cos(k_0 l)$, and on the sine and cosine integral functions of $k_0 l$. Given the experimental uncertainties arising from stray impedances, this theory is a sufficiently good approximation to the most rigorous theory available for the vacuum cylindrical dipole.

It can be seen that the theory reproduces the positions of the maxima and minima well. To achieve this agreement, the sounder dipoles in the model had to be shunted with stray capacitance, in addition to the designed circuit parameters. By trial and error, the best fit was obtained with 20 pF across the long dipole and 42 pF across the short dipole. These capacitances are attributed to contributions from the STEM-dipole motor housing, to a protective collar on a short section of each dipole nearest the spacecraft, and to shunt capacity from the spacecraft body.

The clamping Zener diodes turn on at monitor voltages of about 3.4 V. Above this, where the theoretical shape depends on an approximated diode I–V characteristic, the peak amplitudes are not well reproduced. To further illustrate the importance of the clamping diodes, ISIS I and ISIS II responses for low f_N are plotted together in Fig. 4. Here the 0–10-MHz frequency range gives better resolution of the detail. The ISIS I diodes appear more efficient in restricting the higher voltages than those of ISIS II. In the latter, the monitor voltage exceeds 5.12 V in the 0.1–0.5-MHz range. Below 3.4 V, where the 1N3008 diodes are nonconducting, the two observed responses agree well, illustrating the identical design of the two 400-W amplifiers for operation in their linear domains.

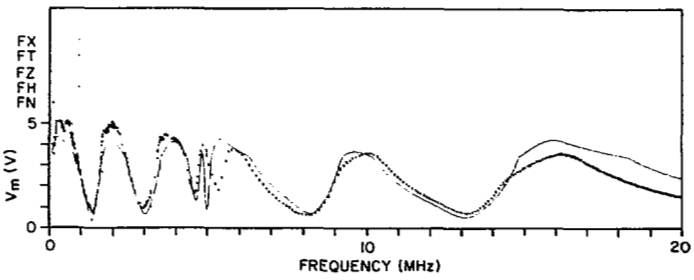

Fig. 3. Monitor voltage V_m as function of frequency. Heavy dots correspond to data and thin line to theory. Short line segments (dots) opposite *FN*, *FH*, *FZ*, *FT*, and *FX* define range bins into which all observational data fall. Data plotted are from ISIS II under low f_N conditions. Vacuum theory in (1) is used.

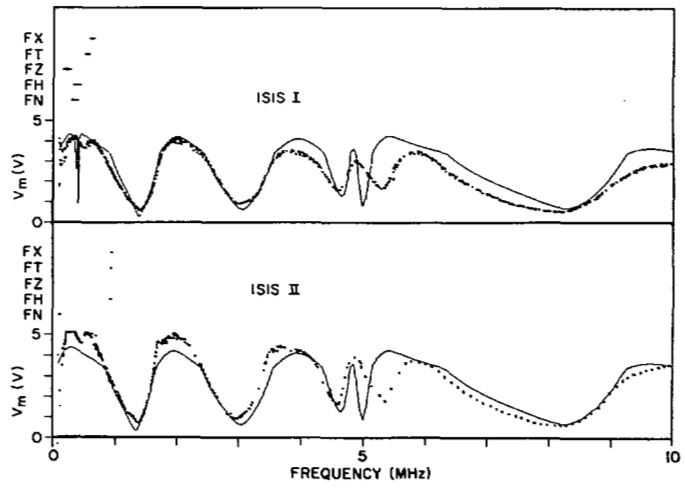

Fig. 4. Comparison of monitor voltage frequency response data from ISIS I and ISIS II under low f_N conditions. Vacuum theory in (1) is used. For other details see caption to Fig. 3.

It is deduced from the goodness of the theoretical fit to the observations that the matching network has been correctly modeled and that the Schelkunoff and Friis [6] impedance theory is adequate for the low-density case. The voltages appearing at the antenna terminals can therefore be calculated with some confidence. The peak amplitudes at both the short and the long dipole terminals, as given by the equivalent circuit analysis, are plotted in Fig. 5. The amplifier is nominally designed to deliver 400 W of pulse power into a matched load of 400 Ω at 1.5 MHz. This corresponds to $V_S = 566$ V. Both panels of Fig. 4 show that voltages much in excess of this are indeed obtained, since V_S approaches $V_m/a = 5/0.005 = 1000$ V at a series of mismatch peaks including 0.3 and 2.0 MHz. The antenna terminal voltage in Fig. 5 achieves similar values at the mismatch peaks; terminal voltage values as high as 1900 V are computed near the antenna crossover frequency of about 5.0 MHz.

B. Results for High Plasma Density

The ISIS I orbit passes through regions of varying density, with the results that f_N values vary from below 0.1 MHz to several megahertz, while f_H values lie in the range 0.5–1.3 MHz. At the ISIS II altitude, f_N rarely exceeds 2.0 MHz, and f_H occupies a narrower range centered near 0.8 MHz. It was found that sorting both data sets by both f_N and f_H removed most of the experimental spread. In the following sections the ISIS II data are presented for specific ranges of f_N and f_H, having regard for antenna orientation. Also the ISIS I data are pre-

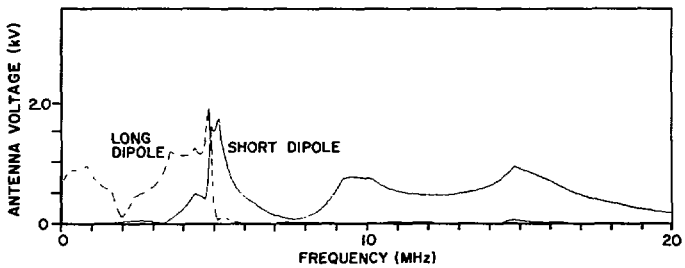

Fig. 5. Theoretical peak voltages at ISIS II antenna terminals for ionospheric parameters in Fig. 3. Vacuum theory in (1) is used.

sented for a wider range of plasma conditions, without distinguishing between orientations.

For theoretical comparison, the transmission line method of Adachi *et al.* [7] was modified to incorporate the effects of a vacuum sheath having a radius s. The dipole capacitance per unit length C was taken to be

$$C = (C_V^{-1} + C_{PL}^{-1})^{-1} \tag{2}$$

in which C_V is the capacitance due to a vacuum cylinder of radius s about the dipole and C_{PL} is the capacitance in a plasma of a dipole of radius s.

The expression developed by Adachi *et al.* [7] for the distributed capacitance per unit length of a dipole of half-length l and radius ρ is

$$C = 2\pi\epsilon_0 F(l, \rho, K, K_0, K') \tag{3}$$

where

$$F(l, \rho, K, K_0, K') = \frac{\sqrt{KK'}}{\log \dfrac{\sqrt{K(Kl^2 + 4K_0\rho^2)} + Kl}{\sqrt{K(Kl^2 + 4K_0\rho^2)} - Kl}}$$

and K, K_0, and K' are functions defined by Adachi *et al.* [7]. Then

$$C_V = 2\pi\epsilon_0[F(l,\rho, 1, 1, 1)^{-1} - F(l, s, 1, 1, 1)^{-1}]^{-1} \tag{4}$$

$$\cong \pi\epsilon_0/\log (s/\rho)$$

and

$$C_{PL} = 2\pi\epsilon_0 F(l, s, K, K_0, K'). \tag{5}$$

The unit arguments in (4) indicate that in a vacuum, $K = K_0 = K' = 1$.

Using the distributed inductance for the dipole $L = \mu_0$ (log $(2l/\rho) - 1)/\pi$, the total impedance Z of the equivalent transmission line can be evaluated as

$$Z = -jZ_0 \cot (kl) = -j\sqrt{L/C} \cot (k_0 lc\sqrt{LC}) \tag{6}$$

where Z_0 is the characteristic impedance of the equivalent transmission line, k is the propagation constant, k_0 is the free-space wavenumber, and c is the speed of light. Expression (6) reduces to an approximation to (1) in the vacuum limit. As f_N, $f_H \to 0$, K, K_0, and $K' \to 1$ and $Z_0 \to -120\,j \cdot \log (l/\rho)$. Then $Z \to -120\,j \cdot \log (l/\rho) \cot/k_0 l)$, the impedance of a transmission line of length l in a vacuum [3, eq. 13-43]. The relationship between the transmission-line theory and the more nearly exact theory leading to (1) is discussed by Schelkunoff and Friis [3]. Expression (6) is essentially the same as one derived by Ament [9] using a different method, and it goes over to one form of the short-dipole impedance [9] for small $k_0 l$ and $s = 0$.

1) ISIS II Data: Results from ISIS II are displayed in Figs. 6 and 7 for selected ranges of f_N, f_H, and (L, B), the angle between the long dipole and the earth's magnetic field direction. The differences between these data and the low density data in Figs. 3 and 4 are significant only between 0 and 2 MHz. When f_N is raised to around 1 MHz, an additional peak appears near f_N with values of voltage comparable to those of the maxima in the low density case. Antenna orientation has a perceptible but relatively unimportant influence on the experimental shape.

The theory reproduces the approximate shape of the observed response, insofar as the frequencies of the maxima and minima are concerned. Also, as can be inferred from the upper and middle theoretical curves in both Figs. 6 and 7, the (L, B) dependence in the range $0^\circ <$ (L, B) $< 60^\circ$ is slight; in fact, there is little difference between the observed distributions in the same two panels.

On the other hand, the details do not match well. Especially in the bottom panels of Figs. 6 and 7, there are theoretical peaks that are not observed in the data. As in the low f_N data of Figs. 3 and 4, the general disagreement for voltages > 3.4 V may be caused by incorrect assumptions about the clamping diodes at the power amplifier output.

When the data represented in Figs. 6 and 7 were sorted according to the value of the angle between the antenna and the satellite velocity vector, the resulting plots were less distinguishable than those in Figs. 6 and 7. The observed variation was thought merely to reflect the (L, B) dependence; most of the data in these cases came from relatively high latitudes where the magnetic field lines were roughly perpendicular to the satellite velocity.

2) ISIS I Data: Fig. 8 is a composite of a set of observed monitor responses selected to illustrate the evolution in response as f_N is increased from about 0.4 MHz to nearly 5.0 MHz. The data displayed are selected from a larger set based on 0.1 MHz intervals in f_N. The experimental spread in various panels of Fig. 8 is caused principally by the use of relatively large f_H bins. In the sequence one sees that, as f_N increases, it pushes with it a perturbation from the vacuum shape that stretches from just above f_N down to the lowest frequencies. The relative sparseness of points in the higher f_N cases, Fig. 8(d), reflects the fact that the ISIS I spacecraft does not spend a large fraction of its time at heights low enough for local f_N to reach these values.

The spacecraft spin vector was at nearly right angles to the orbit plane for all the ISIS I data, and hence there is an almost equal weight for all values of (L, B) between 0° and 90° in the data set. Because of this and because varying (L, B) from 0° to 90° does not change the basic shape of the theoretical curves, the theoretical response for Fig. 8 was evaluated using expression (6) with (L, B) $= 45^\circ$. Throughout most of the panels, the observed and theoretical responses are similar. Their discrepancies in detail have similar magnitudes to those in the ISIS II data in Figs. 6 and 7.

3) Effects of Changing Experimental Conditions: Voltage monitor data from the 100-W amplifier in ISIS I have been processed. The frequency responses from this transmitter for the range $0.1 < f_N < 1.0$ MHz have shapes that are very similar to those found using the 400-W transmitter. The greatest differences between the two data sets are in the detailed shapes near the maxima where the data are probably influenced by

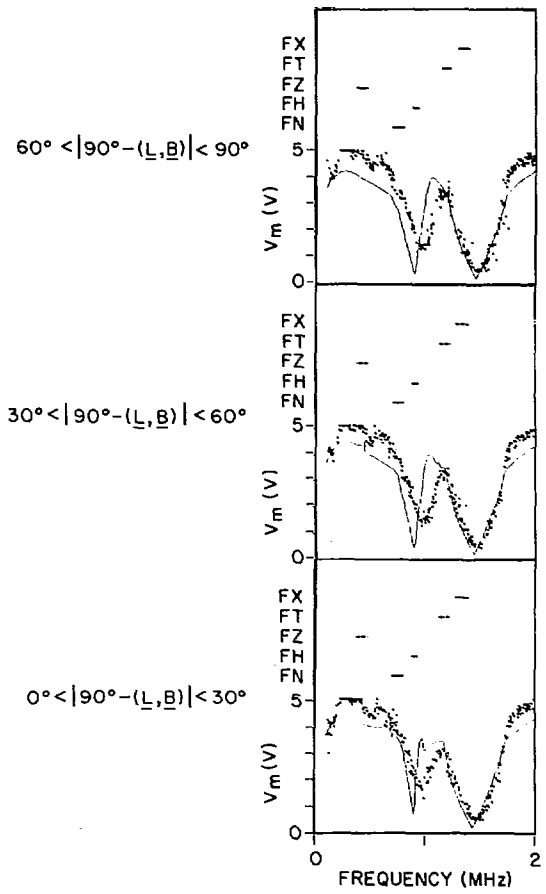

Fig. 6. ISIS II monitor voltage versus frequency for $0.7 \leqslant f_N \leqslant 0.8$ MHz, $0.88 \leqslant f_H \leqslant 0.94$ MHz, and three range bins of (L, B), angle between long sounder dipole and magnetic field. Cold plasma theory in (6) is used. For theoretical curves in top, middle, and bottom panels, (L, B) equals 15°, 45°, and 75°, respectively. f_N and f_H values are given by center of range bin line segments opposite *FN* and *FH*, respectively. For other details, see caption to Fig. 3.

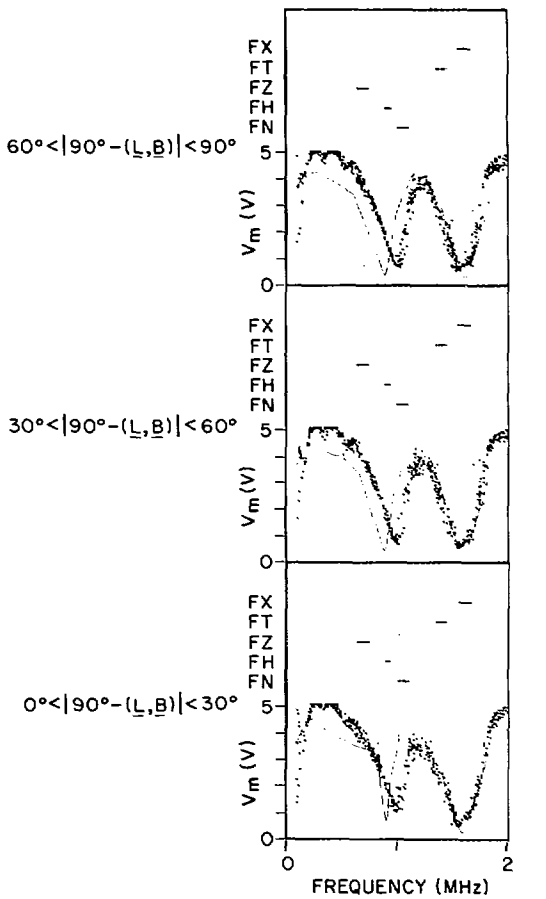

Fig. 7. ISIS II monitor voltage versus frequency for $1.0 \leqslant f_N \leqslant 1.1$ MHz, $0.89 \leqslant f_H \leqslant 0.94$ MHz, and three range bins of (L, B), angle between long sounder dipole and magnetic field. Cold plasma theory in (6) is used. For theoretical curves in top, middle, and bottom panels, (L, B) equals 15°, 45°, and 75°, respectively. f_N and f_H values are given by center of range bin line segments opposite *FN* and *FH*, respectively. For other details, see caption to Fig. 3.

the different characteristics of the clamping diodes in the amplifier output stages. Otherwise, the ratio of the voltage amplitudes from the 100-W and 400-W amplifiers are within five percent of the ratio expected on the basis of the prelaunch calibration of the monitors (2.23 to 1), and the maxima and minima lie at the same frequencies. The fact that the 100-W and 400-W observations are similar, when combined with the qualified success of the transmission-line theory, suggests that the low signal level theory is roughly correct.

The ISIS II responses for specific ranges of f_N for sunlit conditions showed no variations with respect to the responses when the spacecraft was in the dark. The effect of an antenna sheath formed by photoelectrons was thereby shown to be insignificant.

Local RF fields probably increase the dimensions of the antenna sheath significantly. In evaluating (6), the sheath radius was varied as a free parameter to find the best fit. The range $0.1 < s < 1.0$ m gave the best agreement for the ISIS I data, while $1.0 < s < 10$ m worked best with the ISIS II data. Fig. 9 illustrates the theoretical responses for $s = 0.01$, 0.1, 1.0, and 10 m when applied to the same data as in the central panel of Fig. 7. A value of $s = 1.0$ was therefore applied throughout all the theoretical plots. Although the theory was not extremely sensitive to small changes in s, values of $s \cong 1.0$ m definitely yielded more realistic results than $s < 0.1$ m. The existence of an appreciable RF sheath is thus supported.

V. DISCUSSION

Comparison of the highly reproducible voltage-monitor data with an impedance theory indicates that the latter gives approximate agreement in the range $0.1 < f < 5.0$ MHz but that at certain frequencies there is disagreement in the details. From the ISIS experiments there are at least two indications that the RF fields around the antennas create a local environment which is unlike the undisturbed cold plasma background.

1) Details of the Voltage Monitor Response: There are sharp peaks in the theoretical curves for finite f_N at frequencies in the neighborhood of f_N and f_H, but corresponding peaks are absent from the observations. This indicates that the background plasma has been disturbed from its ambient condition. The theoretical peaks relate to the resonance cone singularities in (6) and have been observed in laboratory experiments [10]. Such peaks can be seen in Figs. 6 and 7. For instance, in the middle and lower panels of Fig. 6, there is a "pip" on the theoretical curve at 0.43 and 0.69 MHz, respectively. Although the theoretical pips appear insignificant in the curves plotted, the resonance cone contributes significantly to the theoretical curve shape at frequencies just below the lesser of f_N and f_H, for (L, B) values close to 90°. The data for such frequencies and (L, B) values, and for plasma parameters like those of Figs. 6 and 7, were sorted into (L, B) bins of 5°; the results give little evidence of the resonance cone. Since different manifes-

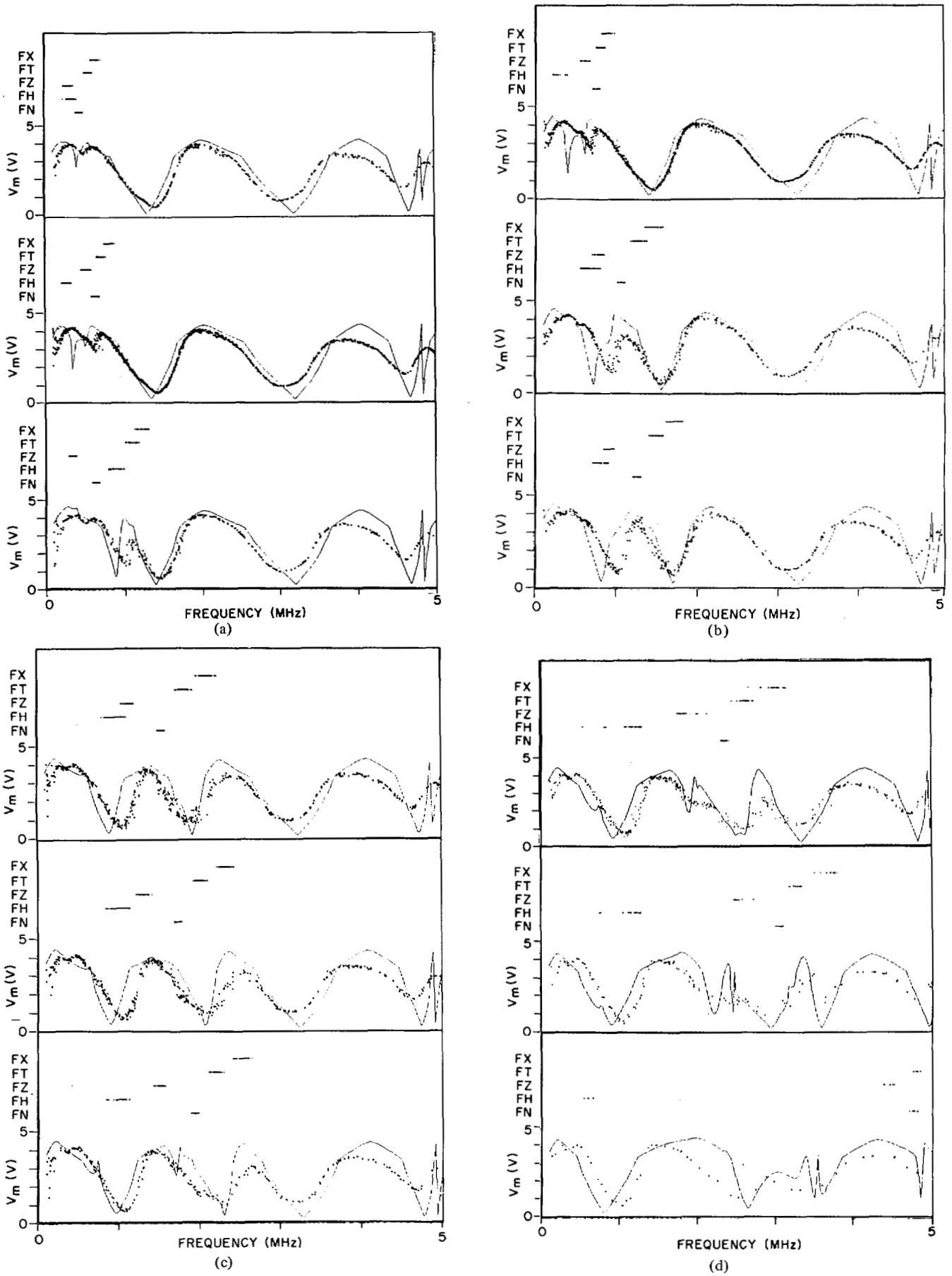

Fig. 8. Series of ISIS I monitor-voltage versus frequency curves to show the change in shape as f_N increases from 0.4 to 4.8 MHz, for selected ranges of f_N and f_H. Cold plasma theory in (6) is used with (**L**, **B**) = 45° throughout. f_N values (MHz) applied to theory are as follows. (a) 0.45, 0.65, and 0.65. (b) 0.75, 1.05, and 1.25. (c) 1.55, 1.75, and 1.95. (d) 2.35, 3.05, and 4.75. Likewise, f_H values are as follows. (a) 0.39, 0.28, and 0.90. (b) 0.30, 0.68, and 0.80. (c) 0.96, 1.00, and 1.18. (d) 1.15, 1.15, and 0.60. For other details, see caption to Fig. 3.

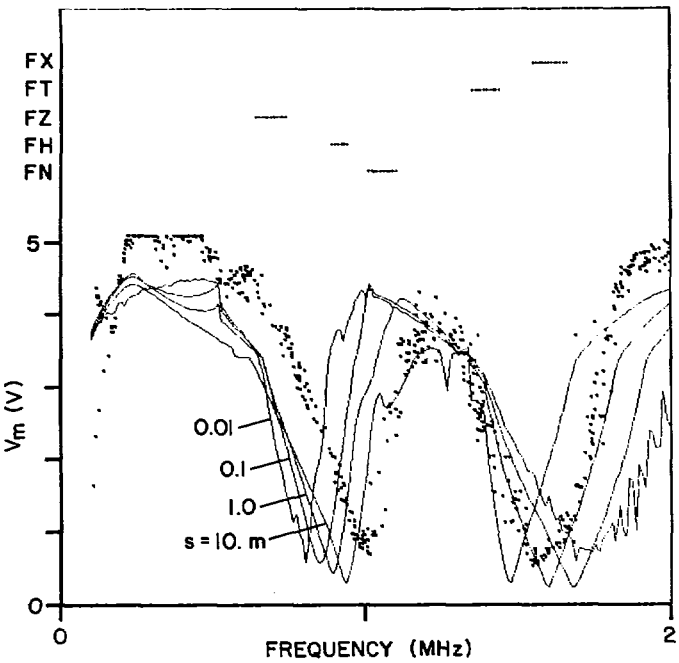

Fig. 9. ISIS II monitor voltage versus frequency for data in middle panel of Fig. 7. Theoretical conditions are same except that four different values of sheath radius s were used to generate theoretical curves.

tations of the cone resonances in the ambient ionospheric plasma have been reported [11], [12], their absence in the present impedance data underlines the dissimilarity between the sounder-excited plasma and the ambient plasma.

2) Plasma Heating by the Sounder: By applying the transmission-line theory to the transmitter equivalent circuit, the voltages appearing across the antenna terminals were computed for the plasma parameters relevant to Figs. 6-8. The peak voltages calculated were commensurate with those obtained in the vacuum case (Fig. 5), about 1 kV. Voltages of this magnitude may cause electric fields of the order of 100 V/m near the spacecraft. The velocity $eE/\omega m$ induced in an electron of charge e and mass m by an oscillating field of amplitude $E = 100$ V/m at a frequency of $\omega = 2\pi \times 10^6$ s^{-1} is 3×10^6 m/s. By comparison, the thermal speed $\sqrt{kT/m}$ of an electron in an equilibrium plasma at $T = 2000$ K is about 0.1 of the induced velocity, and nonlinearities such as the ponderomotive force are expected. The deduced sheath radius of 1 m may be an indication of this nonlinearity.

Large RF fields could heat the ambient particles and, indeed, the soft particle spectrometer on ISIS II does detect sounder-accelerated electrons and protons at energies up to about 1 keV and with total number fluxes S between 10^8 and 10^9 cm^{-2} sr^{-1} s^{-1}, integrated over the 0-10-keV range [13]. Assume that the sounder fields displace electrons isotropically with a flux S from a sphere of radius r during a sounder pulse length τ. The number of electrons displaced per pulse is therefore $S\tau \cdot 4\pi \cdot 4\pi r^2$. A volume of radius r (cm) contains $1.2 \times 10^4 \times 4\pi r^3/3$ ambient electrons when $f_N = 1$ MHz. The ratio of the number of electrons displaced per pulse to the number of ambient electrons in the affected volume is then $100\pi/r$, where r is in centimeters. Even for a moderately large r, this is a further indication that the sounder may radically change the character of the local plasma, and that the heating of the ambient electrons may constitute an important loss mechanism in the calculation of effective impedance at the instant of the RF pulse.

VI. CONCLUSION

Through the use of a model for the ISIS sounder power amplifier, sounder antennas, and associated circuitry, the theory for the impedance of the finite cylindrical dipole in a vacuum is found to be in good agreement with the relevant observations from the low f_N data. This agreement tends to confirm the circuit analysis of the amplifier and the matching network. When modified to include sheath effects, the transmission-line theory for the plasma impedance is found to give fair agreement with the observations, although disagreement is found in the details at certain parts of the total frequency range. An RF sheath radius of about 1 m is deduced from fitting the theory to observations. This result plus the observation of sounder heated particles are evidence that the local plasma is nonlinearly affected by the intense sounder RF fields.

REFERENCES

[1] K. G. Balmain, "The properties of antennas in plasmas," *Ann. Telecommunic.*, vol. 34, pp. 273–283, 1979.
[2] C. D. Florida, "The development of a series of ionospheric satellites," *Proc. IEEE*, vol. 57, pp. 867–875, June 1969.
[3] C. A. Franklin and M. A. Maclean, "The design of swept-frequency topside sounders," *Proc. IEEE*, vol. 57, pp. 897–929, June 1969.
[4] E. L. Hagg, E. J. Hewens, and G. L. Nelms, "The interpretation of topside sounder ionograms," *Proc. IEEE*, vol. 57, pp. 949–959, June 1969.
[5] J. C. Cain and S. J. Cain, "Derivation of the international geomagnetic reference field," NASA Tech. Note TN D-6237, Aug. 1971.
[6] S. A. Schelkunoff and H. T. Friis, *Antennas Theory and Practice*. New York: Wiley, 1952.
[7] S. Adachi, T. Ishizone, and Y. Mushiake, "Transmission line theory of antenna impedance in a magnetoplasma," *Radio Sci.*, vol. 12, pp. 23–31, Jan./Feb. 1977.
[8] W. S. Ament, "Procedures for estimating impedance and radiation properties of ELF/VLF antennas in the ionosphere," in *Proc. Conf. Antennas and Transionospheric Propagation as Related to ELF/VLF Downlink Satellite Communications*, 1970; Naval Res. Lab. Rep. 7462, pp. 40–48, Nov. 1972.
[9] K. G. Balmain, "The impedance of a short dipole antenna in a magnetoplasma," *IEEE Trans. Antennas Propagat.*, vol. AP-12, pp. 605–617, Sept. 1964.
[10] K. Sawaya, T. Ishizone, and Y. Mushiake, "Measurement of the impedance of a linear antenna in a magnetoplasma," *Radio Sci.*, vol. 13, pp. 21–29, Jan./Feb. 1978.
[11] H. G. James, "Spin modulation of high-latitude hiss measured by an electric dipole," *Radio Sci.*, vol. 8, pp. 1133–1147, Dec. 1973.
[12] H. C. Koons, D. C. Pridmore-Brown, and D. A. McPherson, "Oblique resonances excited in the nearfield of a satellite-borne electric dipole antenna," *Radio Sci.*, vol. 9, pp. 541–545, May 1974.
[13] D. M. Klumpar and J. D. Winningham, private communication, 1978.

H. Gordon James was born in Belleville, ON, Canada, on October 8, 1940. He received the B.Sc. degree in engineering physics from Queen's University in 1963 and the M.Sc. and Ph.D. degrees from the University of British Columbia in 1965 and 1968, respectively.

His work has been mainly concerned with the physics of electromagnetic waves in the ionospheric plasma. From 1968 to 1970 he was a Research Associate with the Centre National de la Recherche Scientifique in France; there he studied VLF propagation in the FR-1 satellite program. Since 1970, he has been a Research Scientist with the Communications Research Centre in Ottawa, ON, Canada. His interests have been in investigating various natural and artificial wave processes in the VLF to HF range using the data from the radio experiments on the ISIS spacecraft.

Dr. James is a member of the Canadian Association of Physicists.